



The Concentration of Molecular Nitrogen, Oxygen, Argon and Helium above Dang, Pokhara and Kathmandu Valley, 2020

B. Karki^{1,2*}, S. H. Dhobi^{3,4,5}, J.J. Nakarmi³

¹Department of Physics, Tri-Chandra Multiple Campus, Tribhuvan University, Kathmandu-44600, Nepal

²National Research Council Nepal

³Department of Physics, Patan Multiple Campus, Tribhuvan University, Lalitpur-44700, Nepal

⁴Innovative Ghar Nepal, Lalitpur-44700, Nepal

⁵Robotics Academy of Nepal, Lalitpur-44700, Nepal

*Corresponding author, Email address: magnum.photon@gmail.com

Received 20 Oct 2021,
Revised 18 Dec 2021,
Accepted 19 Dec 2021

Keywords

- ✓ CCMC
- ✓ Dang,
- ✓ Pokhara,
- ✓ Kathmandu,
- ✓ Oxygen,
- ✓ Nitrogen,
- ✓ Helium,
- ✓ Argon.

Bhishma Karki Email:-
magnum.photon@gmail.com

Abstract

The goal of this work is to combine nitrogen, oxygen, argon, and helium above three valleys in Nepal: Dang, Pokhara, and Kathmandu. The observation is made above these valleys due to their high population density and knowledge of gas condensation. One can compare and identify the status of gases, as well as predict the effect of gases that are out of balance with the norm. To study the variation of concentration above Dang, Pokhara, and Kathmandu monthly in 2020, a height of 20km above the earth's surface is taken. The variation of nitrogen, oxygen, Argon and Helium concentration above Dang, Pokhara and Kathmandu vary from 10^{19} molecules. cm^{-3} to 10^{18} molecules. cm^{-3} , 10^{18} molecules. cm^{-3} to 10^{17} molecules. cm^{-3} , 10^{17} molecules. cm^{-3} to 10^{16} molecules. cm^{-3} and 10^{14} molecules. cm^{-3} to 10^{13} molecules. cm^{-3} , respectively. For study authors collect the data from CCMC (Community Coordinated Modeling Center) and data are based on NRLMSISE-00 Atmosphere Model. Furthermore, the observation shows that the concentration of nitrogen gas is highest in February and March, oxygen is highest in February, and argon is highest in January, February, and March above the entire valley. The observation of helium varies and differs from valley to valley; for example, the concentration of helium is high in February above Kathmandu and Pokhara Valleys, but it is highest above Dang Valley in January and February.

1. Introduction

Earth is surrounded by a blanket called atmosphere, which is composed of different reactive and neutral gases, also protect from different radiation coming from the outer atmosphere. Most of the global warming gases like carbon dioxide, ozone, methane, etc. are dense on the lower layer of the atmosphere and increasing day by day due to natural and artificial activities. The lower layer also has dense solid and liquid particles such as dust, smoke, etc. which balance the thermal properties of the atmosphere. The measurement of the composition of gases, particles, etc. at a high altitude takes the help of balloons, rockets, satellites, etc. About 75% of gases lie in a lowermost atmospheric layer called the troposphere. This layer also contains weather system, air pollution, volcanic gases, etc. and the temperature of this layer goes decrease as height increase from the earth surface. The temperature in

this layer decrease with $6.5^{\circ}\text{C}/\text{km}$ at normal condition. The boundary between troposphere and stratosphere is called tropopause with a temperature of about -50°C .

In modern-day about 20.5% of molecular oxygen (O_2) in the atmosphere was also supported by earth photosynthesis both from terrestrial and ocean, about 9×10^{15} mol $\text{O}_2 \text{ y}^{-1}$ was produced by ocean-atmosphere, this is due to the presence of oxygenic phototrophs. It was thought that the abundance of O_2 is less in history than modern for this, the credit goes to a land plantation [1, 2, 3]. The first and most abundant gas in the atmosphere is nitrogen which is about 78% and essential for earth living organisms. This is because nitrogen is a building block of amino acid, protein, enzymes, tissues, antibody formation, hormone production, and another process, with 19ppm [4, 5]. The study of nitrogen distribution globally has low attention than the carbon cycle, the neutral nitrogen gas is extracted from the atmosphere and converted into a different form for artificial use like fertilizer, plastics, explosives, etc., and this Haber-Bosch process is the most used abundance method till. Reactive nitrogen causes nitrogen pollution which affects the environment badly [7, 8].

The troposphere is the closure and lowest layer of the earth's atmosphere which ranges from 0 to 18km in general and this layer is the densest layer of the atmosphere. The phenomena of cloud formation, storms, water vapor, regulating temperature take place in this layer. This layer contains about 99% of water vapor, the concentration of water varies with geographical structure. The mass of mixture gases present in the atmosphere is about 5.15×10^{15} tons and this is due to the gravitational attraction, the mean molecule's mass of air is considered as 28.966 gmol^{-1} . About 99.96% of atmospheric gases are permanent gases like Nitrogen, Oxygen, and Argon. The variation of water from minimum to maximum according to temperature. The mixture of gases up to 100km high from the earth's surface is quite uniform with excluding ozone and water vapor and such a uniform part of the atmosphere is called the homosphere [9]. Control animals subjected to moderate hypoxic-ischemia had lower neuronal survival at 7 days, as well as impaired neurologic function at the juvenile age, when compared to naive animals. Severe hypoxic-ischemic damage resulted in a large cerebral infarction in controls, and three noble gases, argon, helium, and xenon, improved cell survival. When argon and xenon were tested only against more severe hypoxic-ischemic injury, they reduced infarct volume. Furthermore, postinjury body weight was lower in the helium-treated group compared to the naive, control, and other noble gas treatment groups in the moderate insult, whereas it is lower in both the control and helium-treated groups in the severe injurious setting [10].

Carpen et al. studied the effects of atmospheric plasma jet treatments on adults of the red flour beetle, *Tribolium castaneum* (Herbst), and the confused flour beetle, *Tribolium confusum* Jacquelin du Val, in wheat grains. They studied the mortality of insects in response to temperature and plasma exposure by changing the gas (argon, argon/oxygen, and argon/nitrogen mixtures). Argon/Nitrogen plasma treatments resulted in induced mortality, whereas Argon/Oxygen plasma treatments resulted in the introduction of a survival effect. The findings suggested that non-thermal plasma treatments have a high potential for development as alternative methods of chemical insecticide control for storage pests [11]. Argon, like helium, is an inert gas that can be used as a carrier gas for elemental analysis without reacting with the samples being analyzed. It is the third most abundant gas in the atmosphere, accounting for more than twice as much as water vapor. However, argon has a thermal conductivity to nitrogen that is 4.14 times that of helium. Historically, the smaller difference in thermal conductivity between argon and nitrogen made accurate results difficult, implying that argon was unsuitable for nitrogen analysis. Oxygen, nitrogen, and hydrogen were all determined successfully at the same time, with the results of both carrier gases agreeing [12].

Plasma has been used in material synthesis and surface modification since the mid-1970s due to the direct activation of reactant species, particularly for the production of nanomaterials. Because of its noble metal-like properties, tungsten nitride with nanostructures has received a lot of attention for applications in catalysis and electrocatalysis. After 20 minutes of helium plasma and 30 minutes of nitrogen plasma, corresponding to ion fluences of $8.4 \times 10^{25} \text{ m}^{-2}$ and $2.3 \times 10^{26} \text{ m}^{-2}$, respectively, a nano-fuzzy layer with a thickness of 700 nm was formed on the tungsten surface, and the core-shell structured W₂N/W nano fibers have a diameter of around 40 nm. The synthesis of nanostructured W₂N in a plasma environment not only broadens the application of plasma methods, but also provides a simple and universal method for designing materials with varying morphologies and properties [13]. Measurements of the suite of dissolved noble gases (He, Ne, Ar, Kr, and Xe) in seawater hold great promise as diagnostics of air-sea gas exchange, deep-water formation, upwelling, diapycnal mixing, and sea-ice interactions due to their biological and chemical inertness and wide range of properties. Given that the approximate scale of disequilibria for noble gases in most oceanic situations is only a few percent, knowing the noble gas solubilities to 0.1 to 0.2 percent or better is desirable. The solubility concentrations of all five stable noble gases (He, Ne, Ar, Kr, and Xe) in water and seawater in equilibrium with marine air at temperatures ranging from near-freezing to 35 °C and three salinities (0, 20, and 40 PSS78) [14].

Time-resolved atomic and molecular emission spectroscopy was used to investigate the laser-induced plasma chemistry produced during the ablation of graphite targets at atmospheric pressure in air, argon, helium, and nitrogen. The first maximum was explained by the early plasma chemistry produced by the ablated carbon species and the confining background gas, whereas the second maximum was explained by atomic recombination and shock wave-induced plasma plume excitation. When the ablation was produced in different background gases, two major effects were observed. First, the presence of oxygen (21%) in air had no effect on atomic lines; however, the intensity and lifetime of CN emission were significantly reduced when compared to a nitrogen-only atmosphere. The reduction of nitrogen species as reaction partners during the plasma chemistry in air. Secondly, due to the assumed higher plasma temperature in Ar, this gas favored the emission intensity and lifetime of atomic species but hindered the formation of C₂ species [15]. Oxygen aberrations in orifice sensors with helium present have been shown to be caused by an increase in volumetric flow rate caused by a decrease in gas density. The phenomenon poses a safety risk because orifice sensors overestimate the oxygen content and may mislead users into believing they are working in a safe environment. In the case of the orifice sensor used in this test, an oxygen content as low as 18.5 percent may be misinterpreted as a safe working environment. The behavior of two types of oxygen sensors, orifice and membrane, was studied in a controlled experiment. In the helium-air mixture test, the orifice sensor showed a large deviation of up to 13% of the measured reading above the actual oxygen content, whereas the membrane sensor remained accurate to within 3% of the actual value throughout its range [16].

The observation and study variation of concentration of nitrogen and air density is similar while oxygen is different above Nepal. The maximum concentration of nitrogen is found in February and March $4.852 \times 10^{18} \text{ cm}^{-3}$ and minimum in August $4.698 \times 10^{18} \text{ cm}^{-3}$, while the air density is maximum in same month $1.809 \times 10^{19} \text{ cm}^{-3}$ and minimum in July $1.751 \times 10^{19} \text{ cm}^{-3}$. Also, the concentration of oxygen was observed constant and minimum throughout June to September with $1.08 \times 10^{-3} \text{ cm}^{-3}$ while January has a maximum concentration of $1.11 \times 10^{-3} \text{ cm}^{-3}$ [17,18].

1.1. Research area

In this study author select three major valleys of Nepal, they are Dang, Kathmandu, and Pokhara valley. These valleys are the highly populated valley of Nepal which focuses us to study this valley.

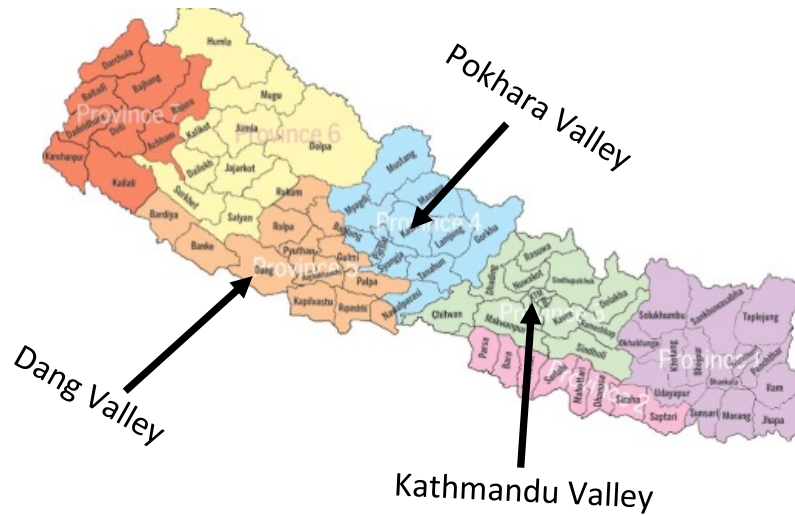


Figure 1. Research Area

2. Methodology

The Community Coordinated Modeling Center (CCMC) is a multi-agency collaboration that provides access to modern space science simulations to the international research community. Furthermore, the CCMC encourages modern space research models to transition to space weather operations. CCMC also provides access to modern space research models to the scientific community via an automated request system for model runs via modern, online visualization and analysis tools via standard data formats for simulation data downloads. NASA Goddard Space Flight Center houses the CCMC (GSFC). The data is collected form CCMC is based on NRLMSISE-00 Atmosphere Model.

A most useful equation to estimate the atmospheric mas with density from sea level to outer space is given as Eqn.1,

$$M_A = \int_0^\infty A \rho dz - \int_0^{f_L} \int_0^{z_L} A \rho dz df \tag{Eqn. 1}$$

Here, $A = A_e \left(1 + \frac{z}{r_e}\right)^2$ and $A_e = 5.10065622 \times 10^{14} m^2$ is the surface area, $r_e = 6,371,007.18 m$, is the radius of a sphere with A_e , ρ is the air density, z is a geometric elevation f_L is a fraction of the earth’s surface area, $z_L =$ elevation at the surface of the land above sea level, which is a function of f WGS84 (2014) and Simpson & Simpson (2020). For dry air as the water, steam behaves like ideal gases, the empirical laws that relate pressure (p), volume (V), and temperature (T):

$$\frac{P_1 V_1}{T_1} = \frac{P_2 V_2}{T_2} \tag{Eqn. 2}$$

The pressure gradient is given as

$$\frac{dP}{dz} = -\rho \times g_n = -\frac{mP g_n}{RT} \tag{Eqn. 3}$$

Here g_n is slandered gravity, ρ is density, z is altitude, P is the pressure, R is the ideal gas constant, T is thermodynamic temperature and m is molar mass.

NRLMSISE-00 empirical atmospheric model based on the ground to exobase which is an upgrade of the MSISE-90 model. The calculate is based on MSIS model parameters and measure the concentration of Atomic oxygen, molecular oxygen, atomic nitrogen, molecular nitrogen, total mass density, neutral temperature, exospheric temperature, Helium, Argon, and Hydrogen atom, etc. NRLMSISE-00, MSISE-90, and Jacchia-70 models are comparable to each other [19]. NRLMSISE-00 model is widely used currently to calculate upper and lower MSIS parameters [20]. The neutral density of gases is calculated using hydrostatic equilibrium and diffusive equilibrium, and expressed root sum of diffusive and mixing densities [21] as,

$$n(z, M) = [n_d(z, M)^A + n_m(z, M)^A]^{\frac{1}{A}} c_1(z) \dots c_n(z) \quad \text{Eqn. 4}$$

$$A = \frac{M_h}{(\bar{M}_0 - M)} \quad \text{Eqn. 5}$$

Here M is the molecular weight of mixture gases, $M_h = 28$, $\bar{M}_0 = 28.95$, n is net number density, n_d is number of density of diffusive profile, n_m is number of density of mixing profile, $c_i(z)$ is lower thermosphere density. Also from equation (4), we have an expression as

$$n_d(z, M) = n_{lb} D(z, M) \left[\frac{T(z_{lb})}{T(z)} \right]^{1+\alpha} \quad \text{Eqn. 6}$$

$$D_B(z, M) = \left[\frac{T(z_{lb})}{T(z)} \right]^{\gamma_2} \exp[-\alpha \gamma_2 \xi(z, z_{lb})] \quad \text{Eqn. 7}$$

$$\gamma_2 = \frac{M g_{lb}}{\left(1 + \frac{z_{lb}}{R_E}\right)^2} \quad \text{Eqn. 8}$$

$$n_{lb} = \bar{n}_{lb} \exp(G(L)) \quad \text{Eqn. 9}$$

Here n_{lb} is the average density at z_{lb} , $g_s = 9.80065 \text{ km/s}^2$, $R_g = 8.314 \times 10^{-3} \text{ g km}^2 / (\text{mols}^2)$, α is thermal diffusion coefficient (He=0.38, Ar=0.17, other =0), the basic expansion formula G(L) for $z \leq 32.5 \text{ km}$ [13].

3. Results and Discussion

The representation in Figure 2-4 below is the observation of concentration of 2020. In this work concentration of major gases (Nitrogen, Oxygen, Argon, and Helium) is present in the troposphere of the atmosphere. The data observation was taken of 12hr in travel, and data are collected from CCMC (Community Coordinated Modeling Center) and data are based on NRLMSISE-00 Atmosphere Model.

3.1 The concentration of Major lower atmospheric gases above Kathmandu Valley in 2020

The observation shows the concentration of molecular nitrogen vary from $2 \times 10^{19} \text{ cm}^{-3}$ to $1.50 \times 10^{18} \text{ cm}^{-3}$ with a high concentration in February and March but a minimum in January. The concentration of molecular Oxygen vary from $5.36 \times 10^{18} \text{ cm}^{-3}$ (molecules. cm^{-3}) to $4.04 \times 10^{17} \text{ cm}^{-3}$ with a high concentration in February but a minimum in January and February. The concentration of Argon vary from $2.39 \times 10^{17} \text{ cm}^{-3}$ to $1.80 \times 10^{16} \text{ cm}^{-3}$ with a high concentration in January, February, and March but a minimum in January and February. The concentration of Helium vary from $1.34 \times 10^{14} \text{ cm}^{-3}$ to $1.01 \times 10^{13} \text{ cm}^{-3}$, with the maximum concentration in February but minimum in January and February. The observation is a picture out in the graph as shown in Figure 2 below and value of E in y-axis is equal to 10^{18} .

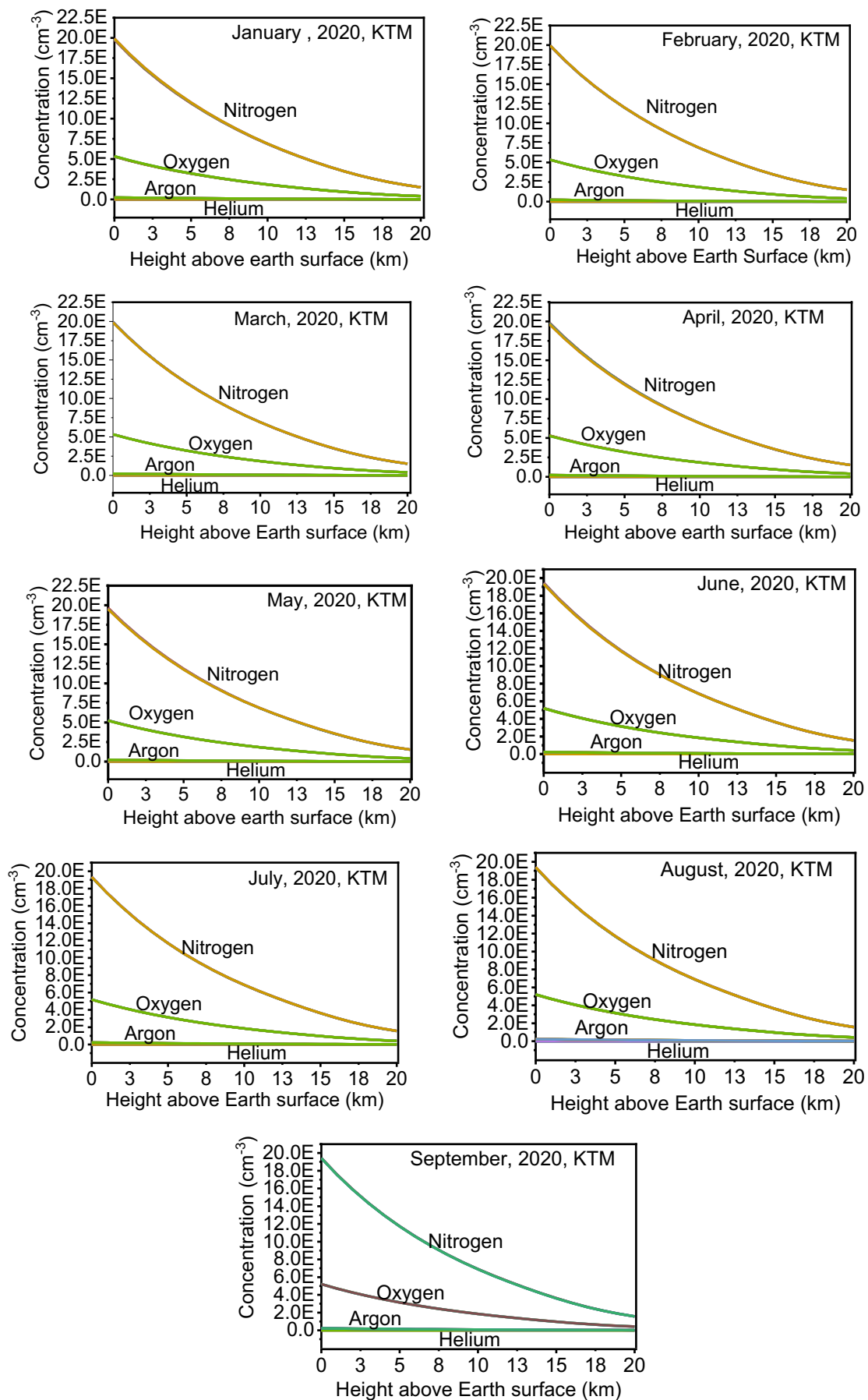
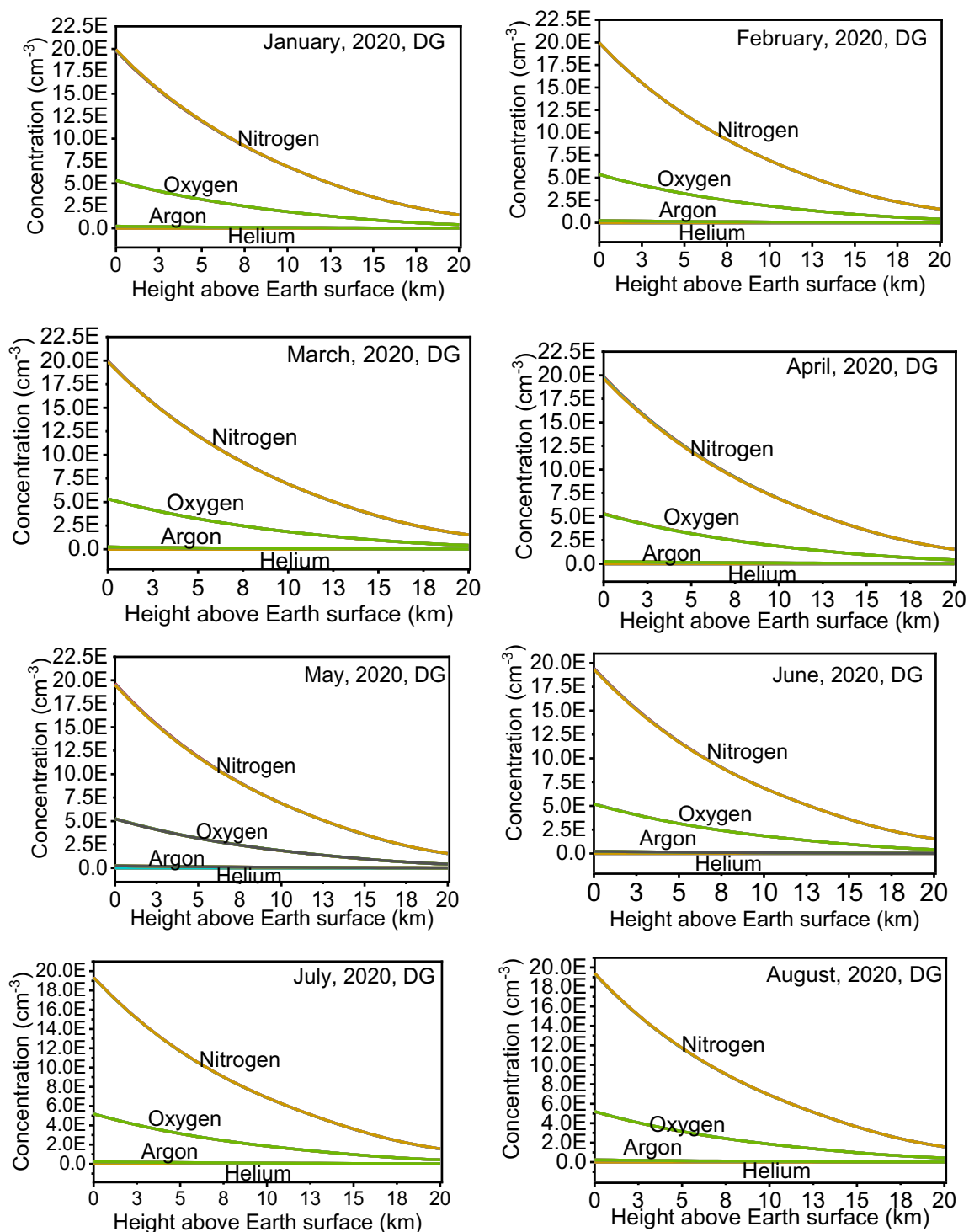


Figure 2. The concentration of tropospheric gas N_2 , O_2 , Ar, He above Kathmandu valley

3.2 The concentration of Major lower atmospheric gases above Dang Valley in 2020

The observation of gas concentration above Dang valley shows the concentration of molecular nitrogen vary from $2 \times 10^{19} \text{ cm}^{-3}$ to $1.50 \times 10^{18} \text{ cm}^{-3}$ with the maximum concentration in February and March but a minimum in January. The concentration of molecular Oxygen vary from $5.36 \times 10^{18} \text{ cm}^{-3}$ to $4.03 \times 10^{17} \text{ cm}^{-3}$ with maximum concentration in February but minimum in January and February. The concentration of Argon is the same as KTM valley Argon concentration. The concentration of Helium vary from $1.34 \times 10^{14} \text{ cm}^{-3}$ to $1.01 \times 10^{13} \text{ cm}^{-3}$ with the maximum concentration in January and February but minimum in January, February, and March. The observation is a picture out in the graph as shown in [Figure 3](#) below.



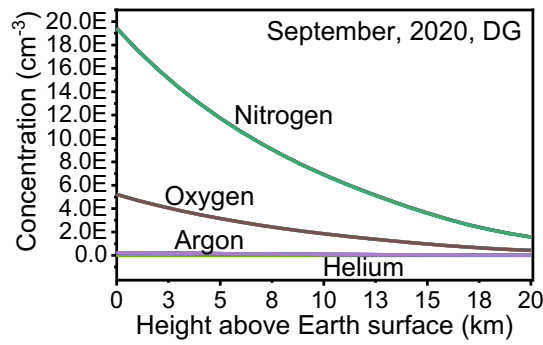
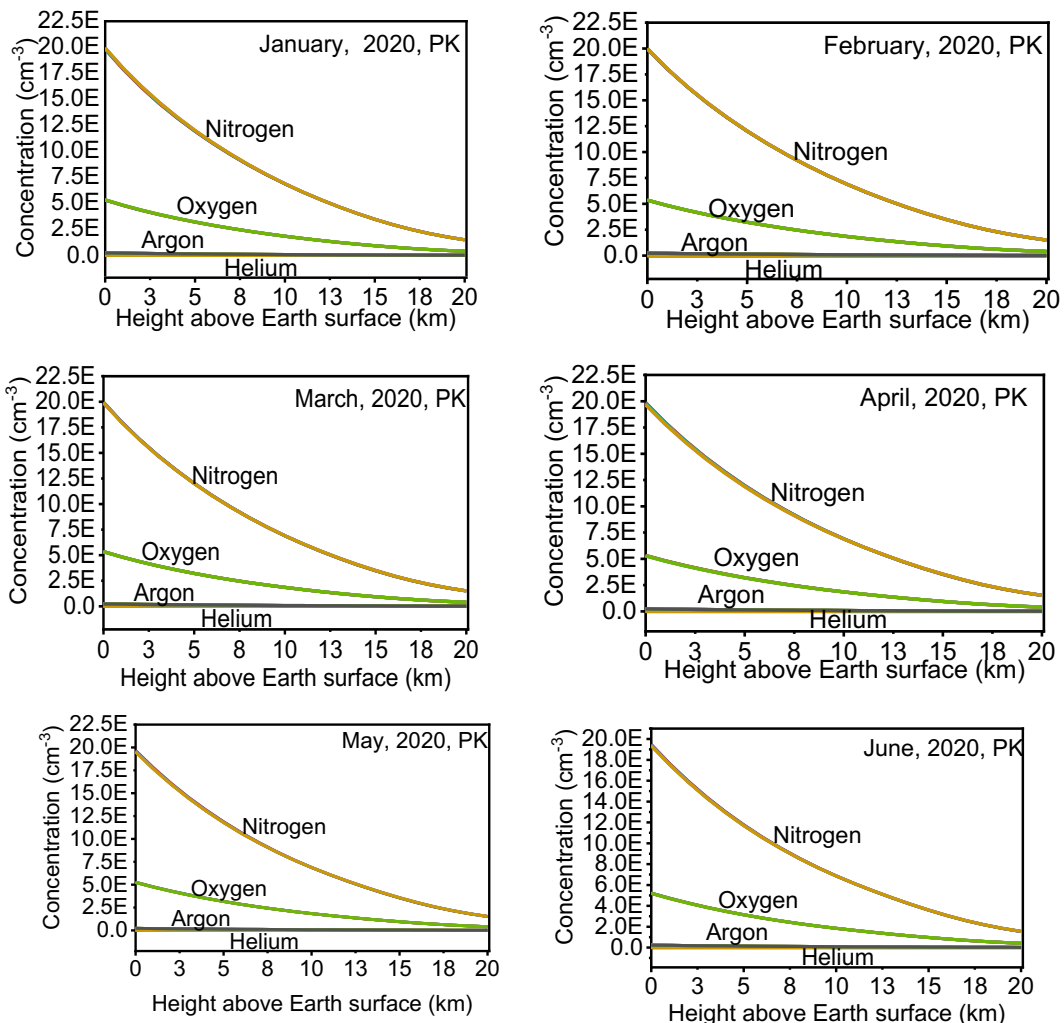


Figure 3. The concentration of tropospheric gas N₂, O₂, Ar, He above Dang valley

3.3 The concentration of Major lower atmospheric gases above Dang Valley in 2020

The observation of gas concentration above Pokhara Valley was observed and the observation shows the concentration of molecular nitrogen above Dang and KTM valley is the same. The concentration of molecular Oxygen ranges vary from $5.36 \times 10^{18} \text{ cm}^{-3}$ to $4.03 \times 10^{17} \text{ cm}^{-3}$ with the maximum concentration in February and March but a minimum in January and February. The concentration of Argon above KTM valley and Pokhara Valley is the same. The concentration of Helium varies ranges from $1.34 \times 10^{14} \text{ cm}^{-3}$ to $1.01 \times 10^{13} \text{ cm}^{-3}$ with the maximum concentration in February but minimum in January, February, and March. The observation is a picture out in the graph as shown in **Figure 4** below.



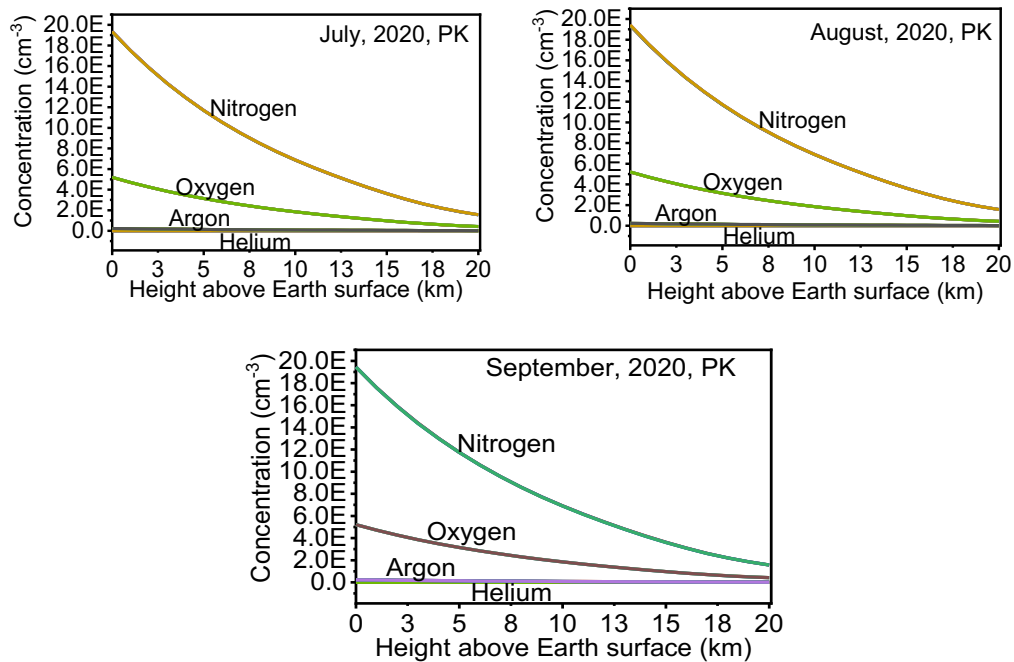


Figure 4. The concentration of tropospheric gas N₂, O₂, Ar, He above Pokhara valley

Table 1-4 gives the detail of variation of gases concentration in the troposphere. **Table 1** shows the variation of molecular nitrogen above Dang, KTM, and Pokhara valley. The concentration of nitrogen gas was maximum in February and March but the minimum is in January above the valleys. Moreover, the gases concentration is high near the earth and low above the earth. For our study, we consider the height from the ground surface of the earth to 20km above the earth's surface.

Table 1. Nitrogen concentration above the valley

Month	The concentration of N ₂ in the troposphere (cm^{-3})		
	KTM Valley	DG Valley	PK Valley
January	1.99×10^{19} to 1.50×10^{18}	1.99×10^{19} to 1.50×10^{18}	1.99×10^{19} to 1.50×10^{18}
February	2.00×10^{19} to 1.51×10^{18}	2.00×10^{19} to 1.50×10^{18}	2.00×10^{19} to 1.50×10^{18}
March	2.00×10^{19} to 1.51×10^{18}	2.00×10^{19} to 1.51×10^{18}	2.00×10^{19} to 1.51×10^{18}
April	1.98×10^{19} to 1.52×10^{18}	1.99×10^{19} to 1.52×10^{18}	1.99×10^{19} to 1.52×10^{18}
May	1.96×10^{19} to 1.53×10^{18}	1.97×10^{19} to 1.53×10^{18}	1.97×10^{19} to 1.53×10^{18}
June	1.95×10^{19} to 1.54×10^{18}	1.95×10^{19} to 1.54×10^{18}	1.95×10^{19} to 1.54×10^{18}
July	1.94×10^{19} to 1.55×10^{18}	1.94×10^{19} to 1.55×10^{18}	1.94×10^{19} to 1.55×10^{18}
August	1.98×10^{19} to 1.57×10^{18}	1.94×10^{19} to 1.57×10^{18}	1.94×10^{19} to 1.56×10^{18}
September	1.94×10^{19} to 1.56×10^{18}	1.95×10^{19} to 1.56×10^{18}	1.95×10^{19} to 1.56×10^{18}

Table 2 shows the variation of molecular oxygen above all Dang, KTM, and Pokhara valley. The concentration of oxygen gas is maximum in February but minimum in January above the valleys. Moreover, the concentration of gases is high near the earth's surface and decreases away from the earth, more detail in **Figure 2-4**.

Table 3: Argon concentration above the valley

Month	The concentration of Ar in the troposphere (cm^{-3})		
	KTM Valley	DG Valley	PK Valley
January	2.39×10^{17} to 1.80×10^{16}	2.39×10^{17} to 1.80×10^{16}	2.39×10^{17} to 1.80×10^{16}
February	2.39×10^{17} to 1.80×10^{16}	2.39×10^{17} to 1.80×10^{16}	2.39×10^{17} to 1.80×10^{16}
March	2.39×10^{17} to 1.81×10^{16}	2.39×10^{17} to 1.81×10^{16}	2.39×10^{17} to 1.81×10^{16}
April	2.37×10^{17} to 1.82×10^{16}	2.37×10^{17} to 1.82×10^{16}	2.38×10^{17} to 1.82×10^{16}
May	2.35×10^{17} to 1.83×10^{16}	2.35×10^{17} to 1.83×10^{16}	2.35×10^{17} to 1.83×10^{16}
June	2.33×10^{17} to 1.85×10^{16}	2.33×10^{17} to 1.84×10^{16}	2.33×10^{17} to 1.84×10^{16}
July	2.32×10^{17} to 1.86×10^{16}	2.32×10^{17} to 1.86×10^{16}	2.32×10^{17} to 1.86×10^{16}
August	2.32×10^{17} to 1.87×10^{16}	2.32×10^{17} to 1.87×10^{16}	2.32×10^{17} to 1.87×10^{16}
September	2.33×10^{17} to 1.87×10^{16}	2.33×10^{17} to 1.87×10^{16}	2.33×10^{17} to 1.88×10^{16}

Table 4. Helium concentration above the valley

Month	The concentration of He in the troposphere (cm^{-3})		
	KTM Valley	DG Valley	PK Valley
January	1.33×10^{14} to 1.01×10^{13}	1.34×10^{14} to 1.01×10^{13}	1.33×10^{14} to 1.01×10^{13}
February	1.34×10^{14} to 1.01×10^{13}	1.34×10^{14} to 1.01×10^{13}	1.34×10^{14} to 1.01×10^{13}
March	1.33×10^{14} to 1.02×10^{13}	1.33×10^{14} to 1.01×10^{13}	1.33×10^{14} to 1.01×10^{13}
April	1.33×10^{14} to 1.02×10^{13}	1.33×10^{14} to 1.02×10^{13}	1.33×10^{14} to 1.02×10^{13}
May	1.31×10^{14} to 1.03×10^{13}	1.32×10^{14} to 1.03×10^{13}	1.32×10^{14} to 1.03×10^{13}
June	1.31×10^{14} to 1.03×10^{13}	1.31×10^{14} to 1.03×10^{13}	1.30×10^{14} to 1.03×10^{13}
July	1.30×10^{14} to 1.04×10^{13}	1.30×10^{14} to 1.04×10^{13}	1.30×10^{14} to 1.04×10^{13}
August	1.30×10^{14} to 1.05×10^{13}	1.30×10^{14} to 1.05×10^{13}	1.31×10^{14} to 1.05×10^{13}
September	1.31×10^{14} to 1.05×10^{13}	1.31×10^{14} to 1.05×10^{13}	1.31×10^{14} to 1.05×10^{13}

Table 3 shows the variation of Argon above Dang, KTM, and Pokhara valleys. The concentration of argon is maximum in January, February, and March but minimum in January and February above the valleys. Moreover, the variation of concentration of argon was also observed as height increase from the surface of the earth. **Table 4** shows the variation of Helium above Dang, KTM, and Pokhara valleys. The concentration of helium is maximum in February but minimum in January and February above the valleys. Moreover, the variation of helium concentration decreased with increasing the height from the earth's surface.

Conclusion

The observation shows the variation of troposphere gases (Nitrogen, Oxygen, Helium, and Argon) concentration depend upon latitude, longitude, gravity, and season. The concentration of gases above the earth's surface is shown in **Figure 2**, **Figure 3**, and **Figure 4** above. The concentration of nitrogen gases vary from $2.00 \times 10^{19} \text{cm}^{-3}$ to $1.50 \times 10^{18} \text{cm}^{-3}$, oxygen from $5.36 \times 10^{18} \text{cm}^{-3}$ to $4.03 \times 10^{17} \text{cm}^{-3}$, argon from $2.39 \times 10^{17} \text{cm}^{-3}$ to $1.80 \times 10^{16} \text{cm}^{-3}$ and helium from $1.34 \times 10^{14} \text{cm}^{-3}$ to $1.01 \times 10^{13} \text{cm}^{-3}$ above the valley in general above the earth's surface at the same height. The concentration of nitrogen gas is maximum in February and March, oxygen in February, argon in January, February, and March above the valley. The concentration of helium concentration is high in February on KTM and PK Valley but the concentration of helium is maximum above DG valley in January and February.

Acknowledgment

The authors would like to thanks all the faculty members of Patan and Tri-Chandra Multiple Campus, Tribhuvan University, Innovative Ghar Nepal, Robotics Academy of Nepal, and National Research Council Nepal for providing different facilities during this work.

Disclosure statement: *Conflict of Interest:* The authors declare that there are no conflicts of interest. *Compliance with Ethical Standards:* This article does not contain any studies involving human or animal subjects.

References

- [1] T. W. Lyons, C. T. Reinhard, and N. J. Planavsky, "The rise of oxygen in Earth's early ocean and atmosphere," *Nature*, 506 (2014) 307-315. doi:10.1038/nature13068.
- [2] T. M. Lenton, et al., "Earliest land plants created modern levels of atmospheric oxygen," *Proceedings of the National Academy of Sciences of the United States of America*, 113 (2016) 9704-9709. doi:10.1073/pnas.1604787113.
- [3] A. J. Krause, et al., "Stepwise oxygenation of the Paleozoic atmosphere," *Nature Communication*, 9 (2018) 4081-4085. doi:10.1038/s41467-018-06383-y.
- [4] C. Pedrolo, Nitrogênio. Centro Universitário Franciscano. (2014). <https://www.infoescola.com/elementosquimicos/nitrogenio/>
- [5] J. R. V. Fogaça, Nitrogênio, (2015). <https://alunosonline.uol.com.br/quimica/nitrogenio.html>
- [6] J.C. Rocha, A. H. Rosa, and A. A. Cardoso, *Introdução à química ambiental*, 2a Ed, Porto Alegre, Artmed, Bookman, (2009).
- [7] M. A. Sutton, et al., *Managing the European Nitrogen Problem: A Proposed Strategy for Integration of European Research on the Multiple Effects of Reactive Nitrogen*, Centre for Ecology and Hydrology and the Partnership for European Environmental Research, (2009).

- [8] European Commission, Nitrogen Pollution and the European Environment Implications for Air Quality Policy, Report, (2013) 2-28.
- [9] K. Mohanakumar, *Stratosphere Troposphere Interactions: Chapter 1 Structure and Composition of the Lower and Middle Atmosphere*, Springer, (2008), 1-252.
- [10] Z. Lei, et al., “The protective profile of argon, helium, and xenon in a model of neonatal asphyxia in rats,” *Critical Care Medicine*, 40(6) (2012) 1724-1730 [doi:10.1097/CCM.0b013e3182452164](https://doi.org/10.1097/CCM.0b013e3182452164)
- [11] L.G. Carpen, et al., “The Effect of Argon/Oxygen and Argon/Nitrogen Atmospheric Plasma Jet on Stored Products Pests,” *Romanian Journal of Physics*, 64(503) (2019) 1-11.
- [12] LECO, “Empowering Results, Oxygen, Nitrogen, & Hydrogen Determination: Helium vs Argon,” <https://info.leco.com/blog/oxygen-nitrogen-and-hydrogen-determination-helium-vs-argon>, accessed at December 15th 2021.
- [13] Z. Wang, et al., “The synthesis of nano-fuzz W2N layer using dense helium and nitrogen plasma,” *Thin Solid Films*, 717(138445) (2021) 123-134. <https://doi.org/10.1016/j.tsf.2020.138445>
- [14] W.J. Jenkins, D.E. Lott, and K.L. Cahill, “A determination of atmospheric helium, neon, argon, krypton, and xenon solubility concentrations in water and seawater,” *Marine Chemistry*, 211 (2019) 94-107. <https://doi.org/10.1016/j.marchem.2019.03.007>
- [15] D. Diaz, and D.W. Hahn, “Plasma chemistry produced during laser ablation of graphite in air, argon, helium and nitrogen,” *Spectrochimica Acta Part B: Atomic Spectroscopy*, 166(105800) (2020) 2-6. <https://doi.org/10.1016/j.sab.2020.105800>
- [16] M. Vanderlaan, and T. Brumm, “Oxygen sensor errors in helium-air mixtures,” *Cryogenics*, 116(103297) (2021), 31-34. <https://doi.org/10.1016/j.cryogenics.2021.103297>.
- [17] S. H. Dhobi, K. Ghimire, D. Kharel, and S. Ghimire, “Variation of Total Mass Density, Oxygen and Nitrogen on Troposphere above Nepal, 2019,” *Journal of Research in Environmental and Earth Sciences*, 7(6) (2021) 48-52.
- [18] B. Karki, S. H. Dhobi, and J. J. Nakarmi, “Study of UV Index above Dang, Pokhara and Kathmandu Valley from 2009 to 2020,” *Journal of Materials and Environmental Science*, 12(5) (2021) 715-727.
- [19] J. M. Picone, A. E. Hedin, and D. P. Drob, “NRLMSISE-00 empirical model of the atmosphere: Statistical comparisons and scientific issues,” *Journal of Geophysical Research*, 107 (2002), 1-2. [doi:10.1029/2002JA009430](https://doi.org/10.1029/2002JA009430).
- [20] X. X. Cheng, et al., “Correction method of the low earth orbital neutral density prediction based on the satellites data and NRLMSISE-00 model” *Chinese Journal of Geophysics*, 56 (2013) 3246–3254.
- [21] A. E. Hedin, “Extension of the MSIS Thermospheric Model into the Middle and Lower Atmosphere,” *Journal of Geophysical Research*, 96 (1991) 1159-1172.

(2021) ; <http://www.jmaterenvirosci.com>